Zirconium Hydride Catalysis Initiated by Tetrabutylammonium Fluoride

Athenea N. Aloiau‡, Briana M. Bobek‡, Kelly E. Pearson‡, Kendall E. Cherry, Christopher R. Smith, John M. Ketcham, Matthew A. Marx, and Stephen J. Harwood*

Mirati Therapeutics, 3545 Cray Court, San Diego, California 92121, United States

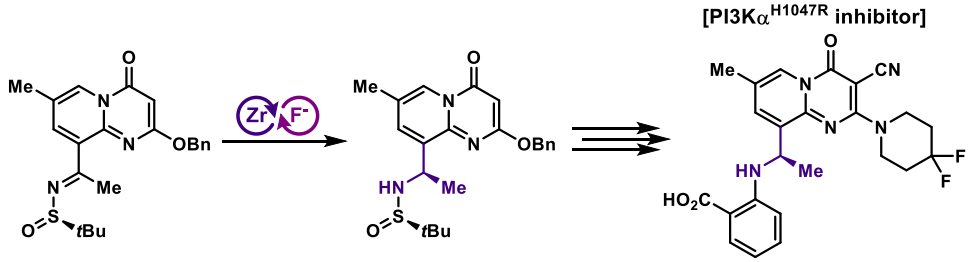

ABSTRACT: In our drug discovery campaigns to target the oncogenic drivers of cancers, the demand for a chemoselective, stereoselective and economical synthesis of chiral benzylamines drove the development of a catalytic zirconium hydride reduction. This methodology uses the inexpensive, bench stable zirconocene dichloride, and a novel tetrabutylammonium fluoride activation tactic to catalytically generate a metal hydride under ambient conditions. The diastereo- and chemoselectivity of this reaction was tested with the preparation of key intermediates from our discovery programs and in the scope of sulfinyl ketimines and carbonyls relevant to medicinal chemistry and natural product synthesis. A preliminary mechanistic investigation conducted into the role of tetrabutylammonium fluoride indicates that formation of a zirconocene fluoride occurs to initiate catalysis. The implications of this convenient activation approach may provide expanded roles for zirconium hydrides in catalytic transformations.

[INTRODUCTION]

Chiral amines frequently appear as motifs in biomolecules,[1] alkaloid natural products,[2] ligands for asymmetric catalysis,[3] and in the structures of synthetically derived active pharmaceutical ingredients (APIs).[4] The chiral benzylamine is a particularly common element in synthetically derived therapeutic agents. Four (repotrectinib,[5] capivasertib,[6] fezolinetant,[7] and iptacopan[8]) of the 34 small molecules in 2023[9] and two (olutasidenib[10] and mavacamten[11]) of the 20 small molecules approved in 2022[12] by the FDA contained a chiral benzylic amine in their structure. As a result of their ubiquity, the synthesis of chiral amines is an active area of synthetic exploration. In our research to discover novel therapeutics targeting oncogenic drivers of cancer we have encountered multiple bioactive chemical series that required a chiral benzylamine element.[13] For example, we developed MRTX0902, a potent, selective, and metabolically stable, clinical-stage inhibitor of the Son of Sevenless 1 (SOS1): KRAS protein-protein interaction (PPI).[14, 15] Over the course of the design and discovery program of SOS1:KRAS PPI inhibitors (**1, Figure 1A**), many diverse enantiopure benzylamine fragments were prepared for attachment onto to the phthalazine core (**2**).

We recently disclosed the discovery and biological activity of a series of pyridopyrimidinone molecules (**3, Figure 1B**) which also contain a chiral benzyl amine. These compounds were found to selectively inhibit the histidine 1047 to arginine Phosphoinositide 3-Kinase alpha (PI3Kα^{H1047R}) mutant protein (**Figure 1B**).[16] Wild-type PI3Kα (PI3Kα^{WT}) plays a crucial role in cellular metabolic processes.[17] It is directly involved in the insulin response and cellular uptake of glucose. As a result, the PI3K-Akt pathway plays a critical role in apoptosis, cellular proliferation, and systemic metabolism. Mutation of the *PIK3CA* gene is an oncogenic driver in many cancers.[18] The specific point mutation of histidine 1047 to arginine is a hotspot with several tens of thousands of breast, colorectal, and endometrial cancer diagnoses each year as a result of this singular mutation. These discoveries have made PI3Kα an attractive target to drug; however, the currently approved therapy indiscriminately inhibits PI3Kα^{WT} and the mutant PI3Kα^{H1047R}.[19] Given the significant role in metabolism that this pathway plays, inhibition of the wild-type protein produces on-target toxicity in the form of hyperglycemia, eventually leading to insulin resistance.[20] To circumvent these issues, researchers have begun focusing on molecules capable of differentiating between the point-mutated protein and wild-type PI3Kα. For all PI3Kα^{H1047R}-specific inhibitor drug discovery programs reported to date, the chiral benzylamine contained in the core is essential to inhibitor activity and selectivity. It forms an intramolecular hydrogen bond with the benzoic acid arranging the acid to directly interact with the point mutated

arginine residue to drive selectivity for PI3Kα^{H1047R} inhibition and avoid the on-target toxicities associated with PI3Kα^{WT} inhibition.[21]

Recently, we shared the development of a convenient method utilizing Schwartz's reagent (zirconocene chloride

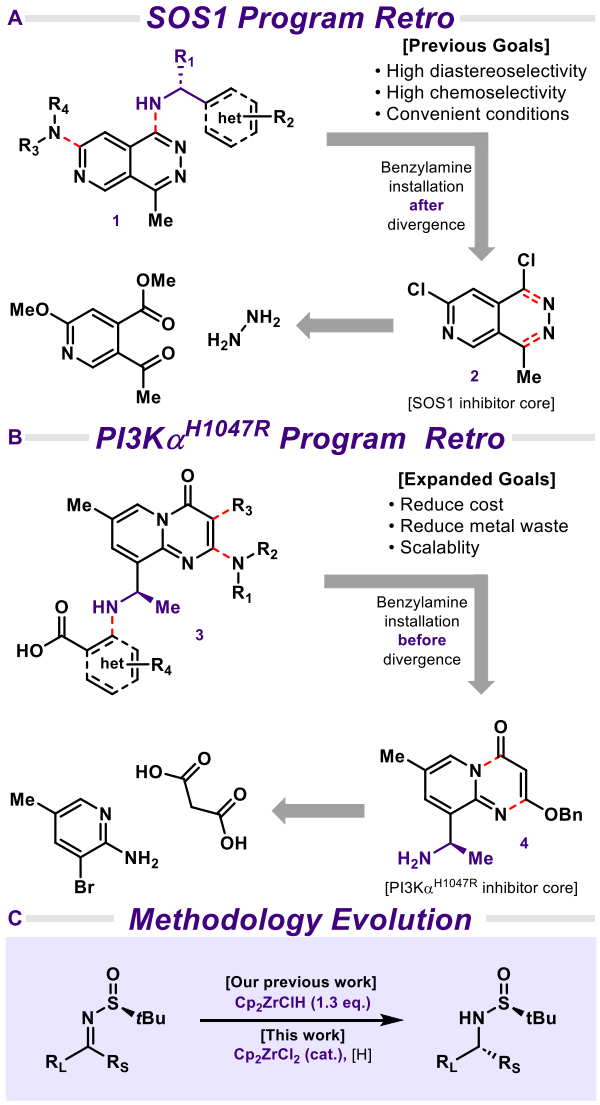

Figure 1. (**A**) Divergent retrosynthetic strategy used in the SOS1:KRAS PPI drug discovery program. (**B**) Divergent retrosynthetic strategy used in the PI3Kα^{H1047R} drug discovery program. (**C**) Research objective to develop a catalytic tactic that would improve both divergent strategies.

hydride, initially reported by Wales and Weingold and developed by Schwartz and coworkers)[22, 23] that was conducted at room temperature and under an ambient atmosphere (**Figure 1C**).[24] Schwartz's reagent proved to be highly diastereoselective in the reduction of chiral sulfinyl ketimines derived from Ellman's auxiliary[25] resulting from its high oxophilicity and bulky cyclopentadienyl ligands. This hydride also proved to be remarkably chemoselective[26] in comparison to many of the conventional metal hydrides applied to the reduction of sulfinyl ketimines (including sodium borohydride, borane, L-Selectride®, lithium triethyl borane, lithium aluminum hydride, diisobutylaluminum hydride). This chemical tactic is well-suited for drug discovery programs, like our SOS1 program, that execute divergent strategies where the chiral benzyl amines are installed onto the molecular core (**2, Figure 1A**).[27, 28] In contrast, the PI3Kα^{H1047R} program utilized a strategy targeting a late-stage Csp^2–N bond formation. Tactically, this implies that the synthesis of the chiral benzylamine motif (**4**) in this program should be introduced onto the core in the linear portion of the synthesis— before the first divergent step. Therefore, we sought to evolve the stoichiometric zirconium hydride methodology into a reaction that would catalytically deploy an inexpensive and bench stable zirconocene complex and use a less costly terminal reductant. We anticipated that utilizing the zirconium catalytically would maintain the high diastereo- and chemoselectivity and convenience previously observed while reducing reaction cost and metallic waste.[29] The development of a catalytic protocol would produce an attractive tactic irrespective of synthetic strategy.

The use of zirconocene complexes as catalysts have found widespread implementation in Lewis acid catalysis,[30] Zeigler-Natta polymerization,[31] and carbometallation chemistry.[32] However, the catalytic use of zirconocene hydrides has historically employed strong reductants (aluminum hydrides) or strong nucleophiles (organolithium, organoalanes, and Grignard reagents).[33] This has limited the utility of catalytic hydrozirconations in synthetic chemistry. An early proof of concept for catalytic reductions using zirconocene complexes with less pyrophoric terminal reductants was reported by Takahashi and Negishi in 1991 (**Figure 2A**).[34] Using three equivalents of ethyl Grignard relative to the zirconocene dichloride, it was possible to generate an activated species proposed to be an alkenyl complex capable of reducing decene to decane under an atmosphere of

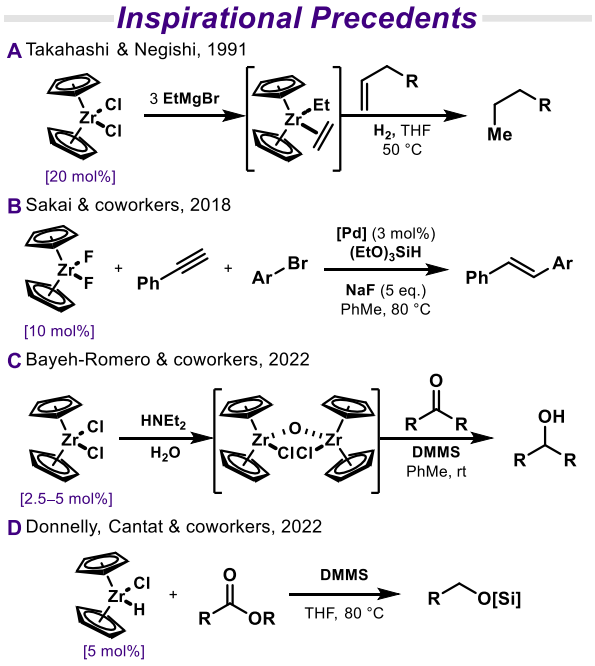

Figure 2. Inspirational precedence to zirconocene catalysis. (**A**) Early example of a catalytic hydrozirconation using a precatalyst activation approach. (**B**) Utilization of a zirconium fluoride precatalyst and sodium fluoride to accomplish catalyst turnover. (**C**) Recent example of a precatalyst activation approach using silane as the terminal reductant. (**D**) Example using an active complex as the catalyst.

hydrogen gas. Silane reagents have been employed previously as the terminal reductant for other group IV metallocene complexes, particularly titanocenes.[35] Interestingly, these early reports utilize metal fluoride metallocene complexes for efficient catalytic activity. In one such recent example from Sakai and coworkers, utilizing either a zirconocene difluoride or hafnocene difluoride, demonstrated the reductive coupling of alkynes and arenes to produce stilbenes (**Figure 2B**).[36] This reaction relies on the use and regeneration of a metal fluoride. Elegant examples deploying commercially available zirconocene complexes and utilizing silanes as terminal reductants have begun to emerge in recent years.[37] In 2022, Bayeh-Romero and coworkers reported that a previously described dimeric complex could be generated in situ and was found to efficiently react with dimethoxymethyl silane (DMMS) to catalytically generate a zirconocene hydride for ketone and ester reduction (**Figure 2C**).[37a] Similarly, in 2022, Donnelly, Cantat and colleagues described the catalytic use of Schwartz's reagent (starting with the requisite hydride ligand) for the catalytic reduction of esters to silyl ethers and alcohols (**Figure 2D**).[37b] These examples suggested that precatalyst activation and catalyst turnover require significant consideration in the development of transformations employing a catalytic zirconocene hydride.

[Results and Discussion]

Using the simple model substrate sulfinyl ketimine (**5**) derived from acetophenone, we began exploring reaction conditions to accomplish a diastereoselective reduction catalyzed by a zirconocene dichloride precatalyst (**Table 1**).

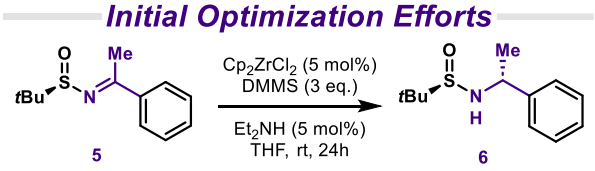

Entry	Deviation	yield[a]
1	no change	6%
2	H_2O (0.5 mol %)	9%
3	H_2O (1.0 mol %)	14%
4	H_2O (2.5 mol %)	13%
5	H_2O (5.0 mol %)	22%
6	No Et_2NH	23%
7	No Et_2NH, H_2O (0.5 mol%)	21%
8	No Et_2NH, H_2O (1.0 mol%)	21%
9	No Et_2NH, H_2O (2.5 mol%)	22%
10	No Et_2NH, H_2O (5.0 mol%)	23%
11	**Cp_2ZrCl_2 (10 mol%), Et_2NH (10 mol%), 48h**	**50%**
12	LiCl (1 eq.)	32%
13	LiCl (1 eq.), H_2O (0.5 mol %)	36%
14	LiCl (1 eq.), H_2O (1.0 mol %)	31%
15	LiCl (1 eq.), H_2O (2.5 mol %)	41%
16	LiCl (1 eq.), H_2O (5.0 mol %)	44%
17	**LiCl (1 eq.), no Et_2NH**	**47%**
18	LiCl (1 eq.), no Et_2NH, 72h	100%

Table 1. Proof of concept for the catalytic, diastereoselective reduction of sulfinyl ketimines using zirconocene dichloride. [a] NMR yield.

We expected this reaction would have two significant challenges to optimization. First, to maintain high diastereoselectivity, we anticipated that we would be unable to increase the reaction temperature to accelerate catalysis. Second, in using a chiral auxiliary that coordinates the catalyst, the resulting reduction product is effectively a bidentate ligand which could result in product inhibition of the catalyst.

We began our exploration of this transformation using the conditions reported in 2022 by Bayeh-Romero and coworkers.[37a] We were excited to find that by increasing the catalyst and amine equivalency to 10 mol% (from 5 mol%) and switching the solvent to the more coordinative ether, tetrahydrofuran (from toluene), resulted in yields up to 50% after two days at room temperature (**Table 1**, entry 11). Further efforts to optimize these reaction conditions proved fruitless. Carefully adjusting the catalyst, water, and amine ratios did not provide improvements in the rate of the reaction. In an attempt to ameliorate any potential product inhibition, lithium chloride was added to the reaction. The introduction of lithium chloride combined with the exclusion of diethylamine and water, provided a 47% yield of **6** after 24h (entry 17). We found that the catalyst was still active at this time and extending the reaction to three days resulted in full conversion of substrate to product (entry 18). These results inspired a campaign to optimize this transformation from the ground up.

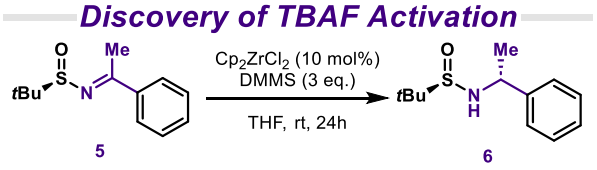

Entry	Deviation	yield[a]
1	no change	17%
2	LiCl (0.5 eq.)	24%
3	LiCl (1.0 eq.)	47%
4	LiCl (2.5 eq.)	45%
5	LiBr (1.0 eq.)	26%
6	LI (1.0 eq.)	N.D.
7	KCl (1.0 eq.)	22%
8	NaCl (1.0 eq.)	20%
9	$ZnCl_2$ (1.0 eq.)	N.D.
10	TBABr (1.0 eq.)	21%
11	TBAF (1.0 eq.)	N.D.
12	**TBAF (1 drop),**	**71%**
13	TBAF (0.1 eq.), LiCl (1 eq.)	98%
14[ref. 24]	Cp_2ZrClH (1.1 eq.), DCM	76%[b]
15	**TBAF (0.13 eq.), LiCl (0.5 eq.), DCM/THF (9/1) [1 gram scale]**	**78%[b] >20:1 dr**

Table 2. Identification of TBAF as a critical additive for catalytic activity. [a] NMR yield. [b] isolated yield. N.D. = not de-

To summarize the results of this second optimization, a variety of common silane reagents were explored, and it was found that silyl ethers are particularly effective in this transformation. The unique reactivity of alkoxysilanes as terminal reductants in other metal hydride systems has been previously explored and a similar effect may be involved in the formation of zirconocene hydrides from silanes.[38] In line with previous findings, DMMS was found to be the most effective reductant (**Table S1**). Several solvents were found to be effective including dichloromethane and toluene, however, tetrahydrofuran was found to give the most catalyst activity and was chosen for early optimization (**Table S2**). Furthermore, the reaction appeared to be relatively insensitive to a range of catalyst loadings and reaction concentrations (**Table S3, S4**). A number of additives were explored including lithium, sodium, potassium and zinc halide salts. Lithium chloride was found to be the most effective salt additive, increasing yield in an equivalent-dependent manner (**Table 2,** entries 2–10). Nevertheless, this reaction still took 3 days to accomplish the full conversion of starting material to product. A breakthrough

came after including tetrabutylammonium fluoride (TBAF) as an additive. At first, one full equivalent was added leading to rapid decomposition of the starting material. Subsequently, a drop of TBAF (1M in THF) was added to the model reaction. After 24 hours, the reaction delivered the desired product in 71% yield (**Table 2,** entry 12). Combining a substochiometric quantity of TBAF (0.1 equivalents) with one equivalent of lithium chloride provided full conversion to product (entry 13). After refining the solvent conditions for diastereoselectivity, full conversion to product could be accomplished using DCM:THF ratio of 9:1 and 10 mol% of the inexpensive, bench stable zirconocene dichloride, 0.13 equivalents of TBAF, and 0.5 equivalents of LiCl. This reaction was performed on gram scale to obtain **6** in a 78% isolated yield with >20:1 dr.

Reaction Refinement

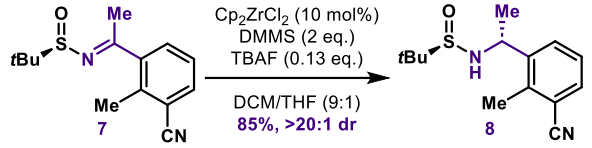

Entry	Deviation	yield[a]	dr
1	No Cp_2ZrCl_2	25%	4 : 1
2	No DMMS	N.D.	—
3	DMMS (1.5 eq.)	57%	> 20 : 1
4	DMMS (3 eq.)	86%	> 20 : 1
5	No TBAF	10%	—
6	TBAF (0.25 eq.)	46%	> 20 : 1
7	**Solid TBAF • $3H_2O$**	**99%**	**> 20 : 1**
8	LiF (0.13 eq.), no TBAF	9%	—
9	NaF (0.13 eq.), no TBAF	11%	—
10	KF (0.13 eq.), no TBAF	13%	—
11	CsF (0.13 eq.), no TBAF	11%	—
12	LiCl (0.5 eq.)	79%	> 20 : 1
13	LiCl (1 eq.)	70%	> 20 : 1
14	0.2 M	83%	> 20 : 1
15	1.0 M	65%	> 20 : 1
16	THF (0.5 M)	70%	> 20 : 1
17	DCM (0.5 M)	75%	> 20 : 1
18[ref. 24]	Cp_2ZrClH (1.1 eq.), DCM	69%[b]	> 20 : 1
19	500mg scale, DMMS (3 eq.)	68%[b]	> 20 : 1

Table 3. Reaction development evaluating fluoride sources as activating reagents. [a] NMR yield. [b] isolated yield. N.D. = not detected.

For a final refinement of the reaction conditions, the more complex model derived from the synthesis of MRTX0902,[14] ketimine **7**, was chosen to increase the dynamic range of the reaction. A series of reactions exploring other fluoride salts, reagent equivalency, solvents, reaction scale, and controls were examined (**Table 3**). A few interesting observations were made throughout the optimization process. A background reaction is present when DMMS is mixed with TBAF that gives sulfinamide **8** in modest yield as a 4:1 ratio of diastereomers (**Table 3**, entry 1).[39] Additionally, when the TBAF is added to a solution of the catalyst and DMMS, gas evolution is observed. If the order of addition is reversed; wherein DMMS is added to a solution of the catalyst and TBAF, then no gas evolution was observed. Solid TBAF works as well (or better) than commercial 1M solutions in THF, although this form of the reagent was found to be less practical for benchtop experimentation due to its hygroscopic nature (**Table 3**, entry 7). Other fluoride salts were found to be ineffective and the amount of TBAF was highly impactful on reaction yield (entries 5–11). Interestingly, the reduction of **7**, in particular, did not benefit from the inclusion of lithium chloride in the same way the reaction of ketimine **5** had (entries 12 and 13). From these observations, we chose to carry forward with two sets of optimized conditions: one using LiCl and one without LiCl during the evaluation of the substrate scope. Two and three equivalents of DMMS were found to be identical on the model substrates, thus, for reaction robustness, 3 equivalents of the silane was chosen for substrate scope exploration.

With a pair of optimal conditions in hand, we applied them to our synthetic problem in the diastereoselective and chemoselective ketimine reduction on the pyridopyrimidinone core (**9**) for our PI3Kα^{H1047R} drug discovery program (**Table 4**).[16a] Like many of the electron deficient heteroaromatic cores found in inhibitors of this class, the pyridopyrimidinone is highly susceptible to reduction. Early in our discovery program several hydride reductants were evaluated for this system. Small, mild reagents like borane gave minimal diastereoselectivity. Large, strong reductants like L-Selectride® exclusively reduced the heterocyclic core. Metal hydrides of moderate reactivity and steric encumbrance, like diisobutylaluminum hydride (DIBAL-H) gave modest selectivity and moderate yields. As a benchmark for the catalytic variant, the stoichiometric reduction using Schwartz's reagent provided a 57% yield of our desired product as a single diastereomer (entry 7). We applied the catalytic reaction (10 mol% Cp_2ZrCl_2, 3 equivalents DMMS, 0.13 equivalents TBAF, 1 equivalent LiCl, 0.4M DCM/THF (9:1) at room temperature) and were pleased to obtain a single diastereomer in 51% isolated yield (entry 8).

Chemoselectivity Profile

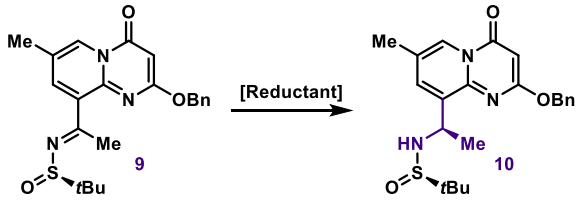

Entry	Conditions	yield[a]	dr
1	$NaBH_4$,-78 °C–rt, THF	37%	2.5 : 1
2	BH_3•DMS,-78 °C–0 °C, THF	61%	1.7 : 1
3	DIBAL-H ,-78 °C–0 °C, THF	52%	2.1 : 1
4	RedAl-H ,-78 °C–0 °C, THF	core reduction	
5	$LiEt_3BH$, -78 °C–0 °C, THF	core reduction	
6	L-Selectride, -78 °C–0 °C, THF	core reduction	
7	Cp_2ZrClH (1.05 eq.), DCM, rt	57%[b]	> 20 : 1
8	**Cp_2ZrCl_2 (cat.), DMMS, TBAF, LiCl**	**51%[b]**	**> 20 : 1**
9	**Entry 8, gram scale**	**47%[b]**	**> 20 : 1**

Table 4. Evaluation for the chemoselectivity and diastereoselectivity of the catalytic reaction applied to the PI3Kα^{H1047R} drug discovery program.[a] NMR yield (combined). [b] isolated yield.

We next evaluated a representative group of sulfinyl ketimines as the substrate scope for this transformation (**Figure 3**). In comparison to the stoichiometric use of Schwartz's reagent, this catalytic reduction exhibited similar characteristics of high functional group tolerance, high chemoselectivity, and high diastereoselectivity.[24] Protic functionalities such as the free aniline (**11**) and phenol (**12**) were well-tolerated — providing higher isolated yields than the stoichiometric use of Schwartz's reagent. Substituting the methyl group on ketimine **5** for an ethyl group (**13**) was

inconsequential on reaction performance; however, substitution for the bulkier isopropyl group led to a reduction in yield and diastereoselectivity (**14**) consistent with the previously reported stoichiometric transformation results. Aryl halides at the ortho-, meta-, and para- positions (**15–17**) are well tolerated. Sensitive 2-bromo and 2-chloropyridine substrates (**18**, **19**) undergo smooth reduction to provide high sulfinamide yields and stereoselectivity without protodehalogenation. The results of unsubstituted pyridines (**20–22**) proved interesting. When the ketimine is in the 2-position diastereoselectivity is significantly impacted without lithium chloride (67% isolated yield, 11:1 dr).

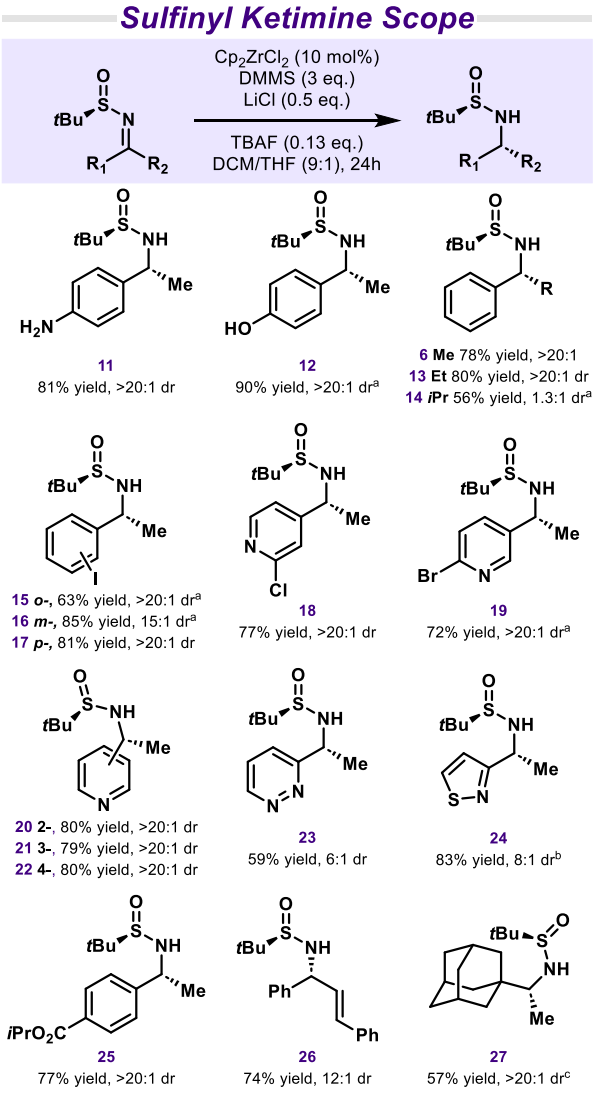

Figure 3. Substrate scope for the diastereoselective reduction of sulfinyl ketimines. Common azines, azoles, protic groups, and electrophilic functionality are all tolerated. [a] no LiCl. [b] 1 eq. LiCl. [c] 48h.

Adding half an equivalent of lithium chloride increased both the yield and selectivity of this reaction, providing **20** in 80% isolated yield with >20:1 diastereoselectivity. This result is recapitulated in the reduction of substrates bearing a pyridazine (**23**) and isothiazole (**24**) where an sp^2-hybridized nitrogen atom is three atoms from the center of reduction. In comparison to the reduction using stoichiometric Schwartz's reagent, this is a meaningful difference in functional group tolerance and is worth consideration in synthetic planning. It is likely that this observation is a result of augmented substrate (or product) coordination to the catalyst. Diastereoselectivity in the reduction of isothiazole **24** was found to benefit substantially from the inclusion of lithium chloride. In the stoichiometric reaction this product was isolated in 36% yield in >20:1 dr. In comparison, the reaction without lithium chloride provided **24** in a 66% yield with a moderate 4.4:1 diastereoselectivity. Adding half an equivalent of lithium chloride improved the yield and selectivity to 74% yield with an 8:1 dr. Further increasing the amount of lithium chloride to a full equivalent improved the yield of **24** to 83% while maintaining an 8:1 dr. Electrophilic functionality such as esters (**25**) and nitriles (**8**) are well tolerated. Unsaturated ketimine (**26**) underwent smooth 1,2-reduction to provide allylic sulfinamides in high yields with reasonable diastereoselectivity (identical to the stoichiometric use of Schwartz's reagent). Alkyl ketimines are also viable substrates, although, the hindered ketimine **27**, bearing an adamantyl group, reacted slowly (48 hours) and in lower yield (57%) in comparison to the stoichiometric variant (80% yield). The impact of steric hinderance is also observed in **14** and **15** where the catalytic reaction was unable to match yield of the stoichiometric transformation at 24 hours. In summary, the catalytic use of the inexpensive and air stable bis(cyclopentadienyl)zirconocene dichloride in the diastereoselective reduction of sulfinyl ketimines provides the desired sulfinamides in yields comparable or higher than the stoichiometric variant with similarly high stereoselectivity. However, results from the reduction of hindered ketimines and heterocycles with Lewis basic nitrogens bearing the ketimine in the 2-position may be improved using the stoichiometric conditions.

We next explored the scope of carbonyl reduction (**Figure 4**). Reductively labile halides (**28–30**) and 2-halopyridines (**31**) are unsurprisingly tolerated under the reaction conditions. Enones and enals are reduced in a 1,2-fashion (**32**). Lastly, seeking to leverage the remarkable steric constraints of the zirconocene hydride catalyst, we imagined it could be possible to selectively reduce molecules bearing multiple carbonyl functionalities in a chemoselective transformation. To test this hypothesis, three commercial steroids bearing commonly found sites of oxidation were reacted under these conditions. Progesterone, bearing three positions for reduction (1,2- and 1,4-reduction of the enone and reduction of the C20 ketone) was selectively reduced to provide the major allylic alcohol isomer **33** in 61% isolated yield. Similarly, 11-oxoprogesterone and adrenosterone, each with four potential sites of reduction, gave 1,2-reduction of the enone providing major allylic alcohol isomers **34** and **35** in 50% and 58% isolated yield, respectively. This tactic compares favorably to the multi-step approach previously developed to accomplish this transformation.[40] This highly chemoselective reduction is performed at room temperature without the need for inert conditions or exclusion of oxygen. The zirconocene hydride is a unique reagent for reduction. It follows the conventional steric approach control model[41] for cyclic ketone reduction and follows the coordinative stereochemical model for ketimine reduction.[42] This zirconocene system also displays the selectivity of large, reactive hydrides and the selectivity of coordinative, mild hydrides depending on substrate context. As a mild and selective transformation, this catalytic

reaction presents an opportunity for late-stage reductions of poly-carbonyl intermediates in natural product synthesis and semi-synthetic drug discovery campaigns. [43]

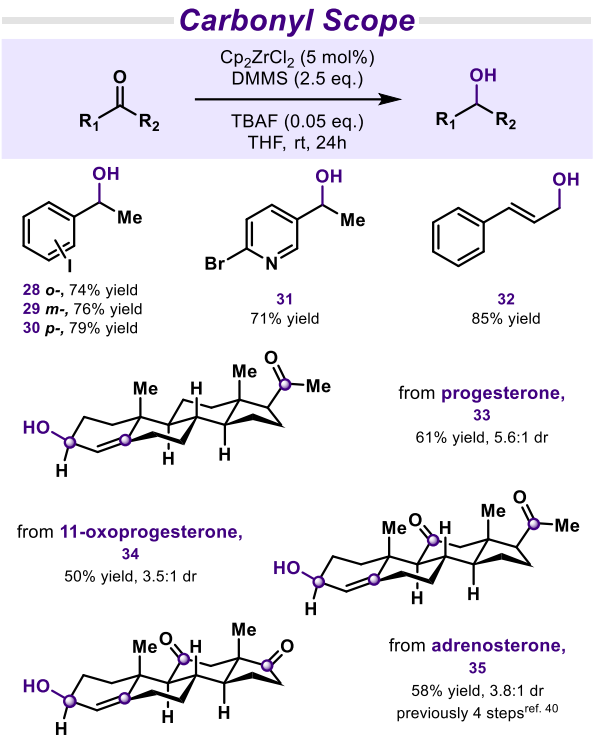

Figure 4. Substrate scope for the chemoselective reduction of ketones.

We sought to understand the critical role of TBAF in this system (**Figure 5A**). As a reagent, tetrabutylammonium fluoride is more sophisticated than its name implies. It is unstable in its anhydrous form; thus, commercial solutions typically contain ~5% water, and as a solid, it is sold as a hydrate. In addition to being a source of highly nucleophilic fluoride, TBAF is a weak base, a phase transfer catalyst capable of solubilizing inorganic ions into organic solvents, and may contain alkyl amines resulting from tetrabutylammonium decomposition.[44] To untangle the role of these variables and gain insight into the mechanism of this diastereoselective reduction we first initiated ^{1}H NMR spectroscopic studies (**Figure S1**). Zirconocene dichloride dissolved in THF-d_8 was exposed to increasing concentrations of TBAF. A reaction was observed and excess TBAF lead to the appearance of unligated cyclopentadiene signals. This is consistent with the observation that an unequal ratio of catalyst to TBAF leads to a loss in catalytic activity (**Table 3**, entry 6). We next conducted a series of experiments using ^{19}F NMR spectroscopy in THF-d_8 (**Figure 5B**). Tetrabutylammonium fluoride (1.0M in THF) was diluted in THF-d_8 and a broad signal was found at –151.63 ppm (spectrum 1). When excess dimethoxy(methyl)silane (DMMS) was reacted with TBAF, a sharp singlet appeared at –94.94 ppm (spectrum 2), indicating that a reaction occurred and a new species was formed, presumably to produce fluorosilicate **36** (**Figure 5A**).[45] Zirconocene difluoride was prepared according to procedure outlined by Sakai and colleagues by reacting Cp_2ZrCl_2 with two equivalents of trimethyltin fluoride.[35h] In THF-d_8, this species exhibited a sharp singlet at 28.70 ppm on the ^{19}F channel (**Figure 5B**, spectrum 3). When treated with 20 equivalents of DMMS, a sharp singlet appeared in just a few minutes at –139.66 ppm (spectrum 4). This is direct evidence that a metathesis reaction between a zirconium fluoride and a silyl hydride can occur. This observed signal is distinct from the fluorosilicate **36** and is instead, likely a silicon fluoride species (such as **37; Figure 5A**). Next, bis(cyclopentadienyl)zirconium dichloride was mixed in an equal molar ratio with TBAF and this mixture was quickly evaluated through ^{19}F NMR. An observable singlet at 66.11 ppm appeared, and the characteristic broad singlet of TBAF at –151.63 ppm is notably absent (**Figure 5B**, spectrum 5). Upon exposing this mixture to excess DMMS the peak at 66.11 ppm disappeared and the previously observed characteristic singlet at –139.56 (**Figure 5B**, spectrum 6) emerged! This data is consistent with the hypothesis that a fluorinated zirconocene species is formed upon the reaction of Cp_2ZrCl_2 and TBAF, and that this complex is distinct from Cp_2ZrF_2. We propose the observed signal at 66.11 ppm corresponds to the mixed halide **38** which is primed to undergo a metathesis reaction with the silyl ether and enter catalysis.

We next evaluated several known and commercial zirconium complexes that potentially serve as precatalysts in this ketimine reduction to further explore this transformation (**Figure 5C**). First, in the absence of catalyst we had previously observed a background reaction (entry 1). In the absence of TBAF and catalyst, the silane reductant is unable to generate product (**Figure 5C**, entry 2). Entry 3 is the standard reaction to provide context. Adjusting the ratio of zirconocene dichloride, we observed empirically that the ratio of TBAF to catalyst is critical. Reducing the catalyst loading (to 5 mol%) gave an 11% yield; however, reducing the TBAF equivalency to match this lower catalyst loading brought the yield up to 53%. These results further corroborated the spectroscopic data and suggest that TBAF interacts with the zirconium center (entries 3-5). Wanting to rule out any phase-transfer behavior of tetrabutylammonium or any possible productive alkylammoium decomposition pathways, we examined several organic salts in lieu of TBAF (entries 6-10). The only two salts that produced any measurable product were the fluoride-containing tetrafluoroborate and hexafluorophosphate alkyl ammonium salts. It has been previously observed that BF_4 salts can produce zirconocene complexes with fluoride ligands and we propose this reactivity likely explains the observed results through either silicon activation or zirconocene activation.[46] Using Schwartz's reagent (Cp_2ZrClH) as the catalyst provided the desired product in 60% yield. This complex already contains a nucleophilic hydride as a ligand. We did not expect this active species to require precatalyst activation. Exposing ketimine **7** to a catalytic amount of Schwartz's reagent in the presence of DMMS as the terminal reductant without the addition of TBAF we observed full conversion of the starting material to sulfinamide **8** (**Figure 5C**, entry 12). This result is consistent with the proposed role of TBAF and the reaction mechanism in **Figure 5A**. Next, we synthesized the bis[chloridoid(cyclopentadienyl)zirconium] oxide [$(Cp_2ZrCl)_2\mu$-O] bimetallic complex and subjected it to a series of control reactions (entries 13–16).[47] It has been previously proposed that this complex, prepared through the reaction of an amine base with water, can serve as an active species in carbonyl reduction.[37a] Commercial solutions of tetrabutylammonium fluoride can contain both water and an amine base. Using this dimeric

complex, we see that the standard reaction, including TBAF, yields 39% desired product (entry 13). Furthermore, adding lithium chloride significantly improves the performance of this precatalyst (entry 14), while the exclusion of TBAF (entries 15 and 16) led to significantly decreased yields. From these findings, we conclude that although TBAF is a source of a weak base and adventitious water, in this catalytic system, it is likely serving a distinct role unrelated to

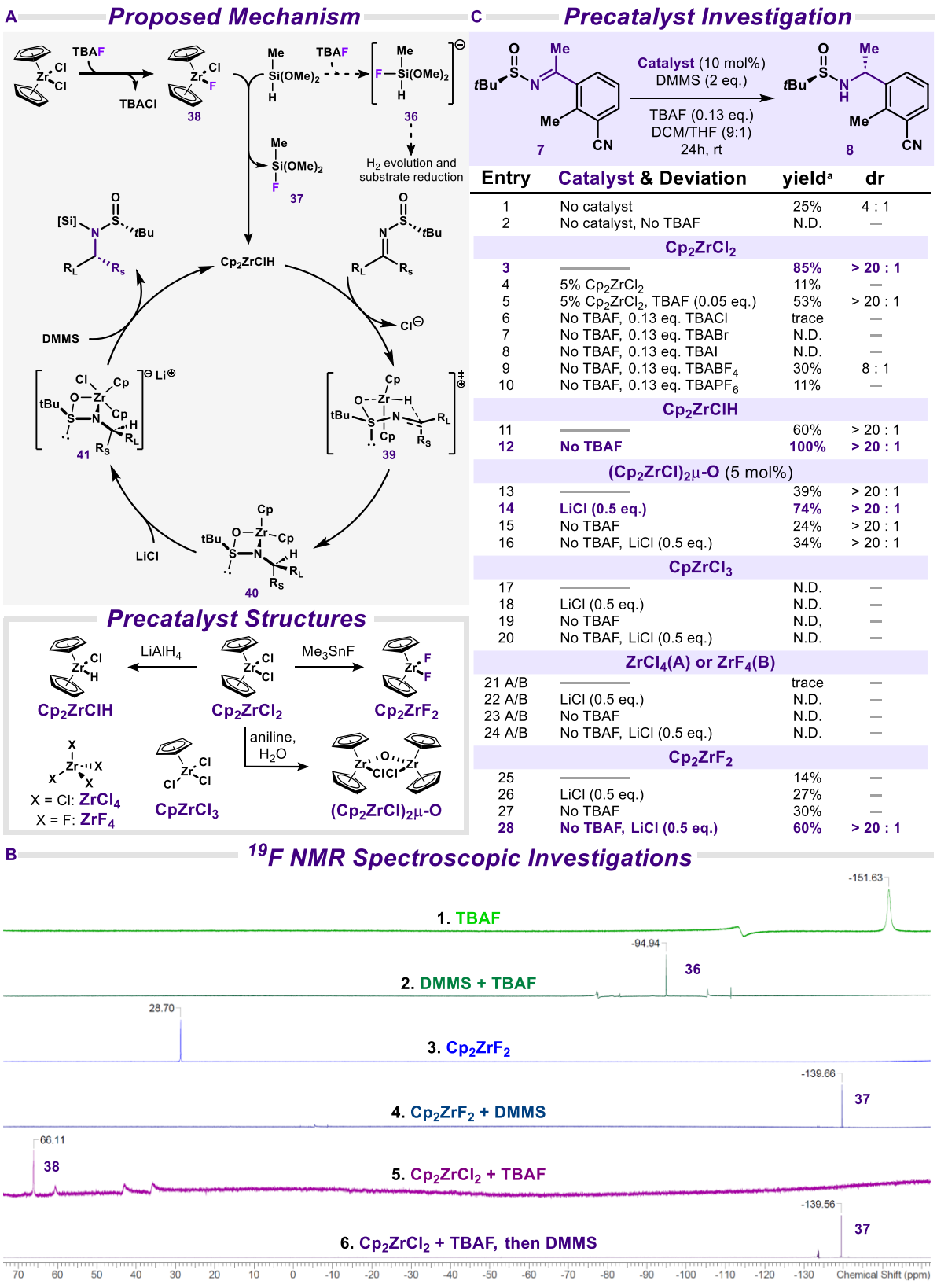

Figure 5. (**A**) Proposed mechanism for the catalytic reduction of sulfinyl ketimines. (**B**) ^{19}F Spectroscopic evidence for the reaction of TBAF with Cp_2ZrCl_2. (**C**) Control experiments evaluating the competency of several zirconium complexes as precatalysts.
[a] NMR Yield N.D. = not detected.

these properties. Based on the ^{1}H spectroscopic results (supporting information, **Figure S2**), it could be hypothesized that disassociation of the cyclopentadienyl ligands (in part, or completely) could produce an active catalyst. Exploring this idea, cyclopentadienylzirconium trichloride ($CpZrCl_3$), bearing one cyclopentadienyl ligand, was introduced into standard control reactions (**Figure 5C**, entries 17-20). This complex was found to be inactive in the attempted reactions. Similarly, zirconium (IV) chloride and zirconium (IV) fluoride ($ZrCl_4$ and ZrF_4, respectively) were each introduced into control reactions. Neither of these complexes produced detectable quantities of product. Lastly, Cp_2ZrF_2 was evaluated for catalytic competency. In the standard reaction a very modest 14% yield was obtained (**Figure 5C**, entry 25). As seen previously with complexes lacking two chloride ligands, introducing lithium chloride to the reaction improved the yield (entry 26), however, this was far from matching the optimized results. Removing TBAF from this system had a significant effect on the catalyst's performance (entries 27 and 28). Removing the external fluoride source and introducing lithium chloride, a 60% yield of a single diastereomer was observed using 10 mol% of Cp_2ZrF_2. We conclude that these results are consistent with the hypothesis that TBAF reacts with Cp_2ZrCl_2 and enables a favorable metathesis reaction between the zirconium fluoride and silane reductant to produce an active zirconocene hydride and a stable silyl fluoride (**Figure 5A**).[35f, 35g]

From all our experimental data, it is clear lithium chloride plays an important role in the reaction. The challenge of product decomplexation from group IV metallocenes has been commented on previously.[35c] Currently, we propose a preliminary mechanism (**Figure 5A**) based on these results and literature support whereby after hydride delivery proceeding through an intramolecular half-chair transition state, (**39**, based on our previous studies)[24] a 4-membered zirconocene complex (**40**) is formed — in accordance with this metal's penchant for 3–5 membered rings.[48] This product-catalyst complex could become turnover limiting. A free halide, presumably chloride in this system, could coordinate to the metal center's available orbital to produce a transient zirconate (**41**; d^0, 18 electron) thereby facilitating product decomplexation and metal hydride reformation (**Figure 5A**).[49] To rationalize the variable benefit of lithium chloride in these reactions, we propose that metallocyclobutanes arising from the reaction of sterically hindered ketimines (for example, those bearing ortho-substitution) may be less stable than those arising from less hindered substrates and, as a result, may benefit less from increasing the concentration of free halide. Lithium chloride could also play a role in catalyst activation either directly, or indirectly, through a counterion exchange equilibrium with TBAF. Further exploration of these possibilities and investigation into the kinetics of this system are the subject of future research.

[CONCLUSION]

In summary, the strategic difference in choreography for the first divergent step and the introduction of the chiral benzylamine in our SOS1 and PI3Kα^{H1047R} drug discovery programs necessitated a methodological improvement for chiral amine synthesis. Both drug discovery programs experienced a critical need to access chiral benzyl amines in high enantiopurities using convenient, functional group tolerant conditions. To address these challenges, a catalytic reaction using an inexpensive, bench stable and commercial precatalyst was developed where initiation was accomplished using a substoichiometric quantity of tetrabutylammonium fluoride. The catalytic generation of a zirconocene hydride enabled an economical synthesis of the pyridopyrimidinone inhibitor core for our PI3Kα^{H1047R} program. This catalytic reaction was tested in the diastereoselective reduction of ketimines relevant to the pharmaceutical industry and in the highly chemoselective carbonyl reductions of functionalized steroid natural products. While selectivities and yields were generally high and in line with the stochiometric reaction, subtle differences in functional group tolerance were uncovered. A mechanistic investigation suggests TBAF is a reagent capable of generating a zirconium fluoride in-situ which promotes active catalyst formation. We expect that this fluoride activation tactic will facilitate the development of other catalytic zirconium hydride transformations where a silane is used as the terminal reductant.

ASSOCIATED CONTENT

• Data Availability Statement

The data underlying this study are available in the published article and its Supporting Information.

• Supporting Information Statement

The Supporting Information is available free of charge on the ACS Publications website.

Synthetic experimental procedures, characterization, and spectral data for compounds **5–35,** zirconium complexes, additional references, discussion, **Tables S1–S15** and **Figures S1–S3**.

AUTHOR INFORMATION

Corresponding Author

* **Stephen J. Harwood** – Mirati Therapeutics, San Diego, California 92121, United States; orcid.org/0000-0003-2127-7239; Phone: 858-461-3546; Email: harwoods@mirati.com

Authors

Athenea N. Aloiau‡ *– Mirati Therapeutics, San Diego, California 92121, United States; orcid.org/0009-0008-0301-9694*

Briana M. Bobek‡ *– Mirati Therapeutics, San Diego, California 92121, United States; orcid.org/0009-0008-7300-9010*

Kelly E. Pearson‡ *– Mirati Therapeutics, San Diego, California 92121, United States; orcid.org/0009-0003-8528-833X*

Kendall E. Cherry *– Mirati Therapeutics, San Diego, California 92121, United States; orcid.org/0009-0007-6931-2853*

Christopher R. Smith *– Mirati Therapeutics, San Diego, California 92121, United States; orcid.org/0000-0002-6553-2791*

John M. Ketcham *– Mirati Therapeutics, San Diego, California 92121, United States; orcid.org/0000-0001-5011-9593*

Matthew A. Marx *– Mirati Therapeutics, San Diego, California 92121, United States; orcid.org/0000-0003-2351-4787*

Author Contributions

SJH: Conceptualization. **ANA, BMB, KEP, KEC, SJH**: Methodology, Investigation, and Formal Analysis. **CRS, JMK, MAM, SJH**:

Writing, Review, and Visualization. All authors have given approval to the final version of the manuscript. ‡These authors contributed equally, and names appear in alphabetical order.

Notes

The authors declare the following competing financial interest(s): All authors of this manuscript are employees of Mirati Therapeutics.

ACKNOWLEDGMENT

The authors are thankful to the Mirati drug discovery and chemical process research and development teams for thoughtful discussion and support. In particular, S. Yu for assistance with ^{19}F NMR and T. Baumgartner for assistance with analytical support. The authors are thankful to M. Achmatowicz, A. Rerick, S. Roshandel, and T. Scattolin for feedback on this manuscript. All research described in this manuscript was funded by Mirati Therapeutics.

REFERENCES

(1) Crick, F. Central dogma of molecular biology. *Nature* **1970**, *227* (5258), 561–563.

(2) (a) Dewick, P. M. *Medicinal Natural Products*; 2001. (b) Kacprzak, K.; Wojaczyńska, E.; Trochimczuk, A.; Steppeler, F.; Wojaczyński, J. Alkaloids as Chiral Building Blocks, Auxiliaries, Ligands, and Molecular Diversity. In *Chiral Building Blocks in Asymmetric Synthesis*, 2022; pp 297–366.

(3) (a) Togni, A.; Venanzi, L. M. Nitrogen Donors in Organometallic Chemistry and Homogeneous Catalysis. *Angew. Chem. Int. Ed. Eng.* **1994**, *33* (5), 497–526. (b) Bennani, Y. L.; Hanessian, S. trans-1,2-Diaminocyclohexane Derivatives as Chiral Reagents, Scaffolds, and Ligands for Catalysis: Applications in Asymmetric Synthesis and Molecular Recognition. *Chem. Rev.* **1997**, *97* (8), 3161–3196. (c) Lucet, D.; Le Gall, T.; Mioskowski, C. The Chemistry of Vicinal Diamines. *Angew. Chem. Int. Ed.* **1998**, *37* (19), 2580–2627. (d) Fache, F.; Schulz, E.; Tommasino, M. L.; Lemaire, M. Nitrogen-containing ligands for asymmetric homogeneous and heterogeneous catalysis. *Chem. Rev.* **2000**, *100* (6), 2159–2232. (e) Juaristi, E.; Anaya de Parrodi, C. Chiral 1,2-Amino Alcohols and 1,2-Diamines Derived from Cyclohexene Oxide: Recent Applications in Asymmetric Synthesis. *Synlett* **2006**, *2006* (17), 2699–2715. (f) Douthwaite, R. E. Metal-mediated asymmetric alkylation using chiral N-heterocyclic carbenes derived from chiral amines. *Coord. Chem. Rev.* **2007**, *251* (5–6), 702–717. (g) Kizirian, J. C. Chiral tertiary diamines in asymmetric synthesis. *Chem. Rev.* **2008**, *108* (1), 140–205.

(4) (a) Lin, G.-Q. Y., Q.-D.; Cheng, J.-F. *Chiral Drugs: Chemistry and Biological Action*; 2011. (b) Tamatam, R.; Shin, D. Asymmetric Synthesis of US-FDA Approved Drugs over Five Years (2016–2020): A Recapitulation of Chirality. *Pharmaceuticals (Basel)* **2023**, *16* (3).

(5) Drilon, A.; Ou, S. I.; Cho, B. C.; Kim, D. W.; Lee, J.; Lin, J. J.; Zhu, V. W.; Ahn, M. J.; Camidge, D. R.; Nguyen, J.; et al. Repotrectinib (TPX-0005) Is a Next-Generation ROS1/TRK/ALK Inhibitor That Potently Inhibits ROS1/TRK/ALK Solvent- Front Mutations. *Cancer Discov.* **2018**, *8* (10), 1227–1236.

(6) Addie, M.; Ballard, P.; Buttar, D.; Crafter, C.; Currie, G.; Davies, B. R.; Debreczeni, J.; Dry, H.; Dudley, P.; Greenwood, R.; et al. Discovery of 4-amino-N-[(1S)-1-(4-chlorophenyl)-3-hydroxypropyl]-1-(7H-pyrrolo[2,3-d]pyrimidin-4-yl)piperidine-4-carboxamide (AZD5363), an orally bioavailable, potent inhibitor of Akt kinases. *J. Med. Chem.* **2013**, *56* (5), 2059–2073.

(7) Hoveyda, H. R.; Fraser, G. L.; Dutheuil, G.; El Bousmaqui, M.; Korac, J.; Lenoir, F.; Lapin, A.; Noel, S. Optimization of Novel Antagonists to the Neurokinin-3 Receptor for the Treatment of Sex-Hormone Disorders (Part II). *ACS Med. Chem. Lett.* **2015**, *6* (7), 736–740.

(8) Schubart, A.; Anderson, K.; Mainolfi, N.; Sellner, H.; Ehara, T.; Adams, C. M.; Mac Sweeney, A.; Liao, S. M.; Crowley, M.; Littlewood-Evans, A.; et al. Small-molecule factor B inhibitor for the treatment of complement-mediated diseases. *Proc. Natl. Acad. Sci. U S A* **2019**, *116* (16), 7926–7931.

(9) de la Torre, B. G.; Albericio, F. The Pharmaceutical Industry in 2023: An Analysis of FDA Drug Approvals from the Perspective of Molecules. *Molecules.* **2024**, *29* (3).

(10) Caravella, J. A.; Lin, J.; Diebold, R. B.; Campbell, A. M.; Ericsson, A.; Gustafson, G.; Wang, Z.; Castro, J.; Clarke, A.; Gotur, D.; et al. Structure-Based Design and Identification of FT-2102 (Olutasidenib), a Potent Mutant-Selective IDH1 Inhibitor. *J. Med. Chem.* **2020**, *63* (4), 1612–1623.

(11) Green, E. M.; Wakimoto, H.; Anderson, R. L.; Evanchik, M. J.; Gorham, J. M.; Harrison, B. C.; Henze, M.; Kawas, R.; Oslob, J. D.; Rodriguez, H. M.; et al. A small-molecule inhibitor of sarcomere contractility suppresses hypertrophic cardiomyopathy in mice. *Science.* **2016**, *351* (6273), 617–621.

(12) (a) Benedetto Tiz, D.; Bagnoli, L.; Rosati, O.; Marini, F.; Santi, C.; Sancineto, L. FDA-Approved Small Molecules in 2022: Clinical Uses and Their Synthesis. *Pharmaceutics.* **2022**, *14* (11). (b) Mullard, A. 2022 FDA approvals. *Nat. Rev. Drug. Discov.* **2023**, *22* (2), 83–88.

(13) (a) Fell, J. B.; Fischer, J. P.; Baer, B. R.; Blake, J. F.; Bouhana, K.; Briere, D. M.; Brown, K. D.; Burgess, L. E.; Burns, A. C.; Burkard, M. R.; et al. Identification of the Clinical Development Candidate MRTX849, a Covalent KRAS(G12C) Inhibitor for the Treatment of Cancer. *J. Med. Chem.* **2020**, *63* (13), 6679–6693. (b) Daemen, A.; Sun, J. D.; Pankov, A.; Duong, F. L.; Yuen, N.; Barkund, S.; Kaushik, S.; Chang, J. H.; Briere, D. M.; Sudhakar, N.; et al. Abstract 1131: ORIC-944, a potent and selective allosteric PRC2 inhibitor, demonstrates robust in vivo activity in prostate cancer models. *Cancer Research* **2021**, *81* (13_Supplement), 1131–1131. (c) Wang, X.; Allen, S.; Blake, J. F.; Bowcut, V.; Briere, D. M.; Calinisan, A.; Dahlke, J. R.; Fell, J. B.; Fischer, J. P.; Gunn, R. J.; et al. Identification of MRTX1133, a Noncovalent, Potent, and Selective KRAS(G12D) Inhibitor. *J. Med. Chem.* **2022**, *65* (4), 3123–3133. (d) Smith, C. R.; Aranda, R.; Bobinski, T. P.; Briere, D. M.; Burns, A. C.; Christensen, J. G.; Clarine, J.; Engstrom, L. D.; Gunn, R. J.; Ivetac, A.; et al. Fragment-Based Discovery of MRTX1719, a Synthetic Lethal Inhibitor of the PRMT5*MTA Complex for the Treatment of MTAP-Deleted Cancers. *J. Med. Chem.* **2022**, *65* (3), 1749–1766. (e) Chen, C. Y.; Lu, Z.; Scattolin, T.; Chen, C.; Gan, Y.; McLaughlin, M. Synthesis of Adagrasib (MRTX849), a Covalent KRAS(G12C) Inhibitor Drug for the Treatment of Cancer. *Org. Lett.* **2023**, *25* (6), 944–949. (f) Snead, D. R.; Gan, Y.; Scattolin, T.; Paymode, D. J.; Achmatowicz, M.; Rudisill, D. E.; Vidal, E. S.; Gharbaoui, T.; Roberts, P.; Yang, J.; et al. Development of Adagrasib's Commercial Manufacturing Route. *Organic Process Research & Development* **2023**, *27* (3), 530–538.

(14) (a) Ketcham, J. M.; Haling, J.; Khare, S.; Bowcut, V.; Briere, D. M.; Burns, A. C.; Gunn, R. J.; Ivetac, A.; Kuehler, J.; Kulyk, S.; et al. Design and Discovery of MRTX0902, a Potent, Selective, Brain-Penetrant, and Orally Bioavailable Inhibitor of the SOS1:KRAS Protein-Protein Interaction. *J. Med. Chem.* **2022**, *65* (14), 9678–9690. (b) Scattolin, T.; Lizza, J. R.; Xu, Z.; Zhao, D.; Chen, C.-y. Process Development and Scale-Up of the SOS1 Inhibitor MRTX0902. *Organic Process Research & Development* **2023**, *27* (6), 1061–1068.

(15) (a) Boriack-Sjodin, P. A.; Margarit, S. M.; Bar-Sagi, D.; Kuriyan, J. The structural basis of the activation of Ras by Sos. *Nature.* **1998**, *394* (6691), 337–343. (b) Jeng, H. H.; Taylor, L. J.; Bar-Sagi, D. Sos-mediated cross-activation of wild-type Ras by oncogenic Ras is essential for tumorigenesis. *Nat. Commun.* **2012**, *3*, 1168. (c) Kessler, D.; Gerlach, D.; Kraut, N.; McConnell, D. B. Targeting Son of Sevenless 1: The pacemaker of KRAS. *Curr. Opin. Chem. Biol.* **2021**, *62*, 109–118. (d) Sheffels, E.; Kortum, R. L. Breaking Oncogene Addiction: Getting RTK/RAS-Mutated Cancers off the SOS. *J. Med. Chem.* **2021**, *64* (10), 6566–6568.

(16) (a) Ketcham, J. M.; Harwood, S. J.; Aranda, R.; Aloiau, A. N.; Bobek, B. M.; Briere, D. M.; Burns, A. C.; Caddell Haatveit, K.; Calinisan, A.; Clarine, J.; et al. Discovery of Pyridopyrimidinones that Selectively Inhibit the H1047R PI3Kalpha Mutant Protein. *J. Med. Chem.* **2024**, *67* (6), 4936–4949. (b) Ketcham, J. M. S., C. R.; Marx, M. A.; Lawson, J. D.; Harwood, S. J.; Burns, A. C.; Caddell-Haatveit, K.; Pearson, K. E.; Aloiau, A. N. G.; Kuehler, J.; Bobek, B. ;

Watkins, A. H.; Jones, B. D.; Ivetac, A. D.; Wang, X. Substituted Pyridopyrimidinones. WO2024044769, 2024.
(17) (a) Jean, S.; Kiger, A. A. Classes of phosphoinositide 3-kinases at a glance. *J. Cell. Sci.* **2014**, *127* (Pt 5), 923–928. (b) Cantley, L. C. The phosphoinositide 3-kinase pathway. *Science.* **2002**, *296* (5573), 1655–1657.
(18) (a) Stemke-Hale, K.; Gonzalez-Angulo, A. M.; Lluch, A.; Neve, R. M.; Kuo, W. L.; Davies, M.; Carey, M.; Hu, Z.; Guan, Y.; Sahin, A.; et al. An integrative genomic and proteomic analysis of PIK3CA, PTEN, and AKT mutations in breast cancer. *Cancer Res.* **2008**, *68* (15), 6084–6091. (b) Samuels, Y.; Waldman, T. Oncogenic mutations of PIK3CA in human cancers. *Curr. Top. Microbiol. Immunol.* **2010**, *347*, 21–41. (c) Hoxhaj, G. M., B. D. The PI3K-AKT network at the interface of oncogenic signalling and cancer metabolism. *Nat. Rev. Cancer* **2020**, *20* (2), 74–88. (d) Jiang, N.; Dai, Q.; Su, X.; Fu, J.; Feng, X.; Peng, J. Role of PI3K/AKT pathway in cancer: the framework of malignant behavior. *Mo.l Biol. Rep.* **2020**, *47* (6), 4587–4629. (e) Reinhardt, K.; Stuckrath, K.; Hartung, C.; Kaufhold, S.; Uleer, C.; Hanf, V.; Lantzsch, T.; Peschel, S.; John, J.; Pohler, M.; et al. PIK3CA-mutations in breast cancer. *Breast Cancer Res. Treat.* **2022**, *196* (3), 483–493.
(19) (a) Andre, F.; Ciruelos, E.; Rubovszky, G.; Campone, M.; Loibl, S.; Rugo, H. S.; Iwata, H.; Conte, P.; Mayer, I. A.; Kaufman, B.; et al. Alpelisib for PIK3CA-Mutated, Hormone Receptor-Positive Advanced Breast Cancer. *N. Engl. J. Med.* **2019**, *380* (20), 1929–1940. (b) Zhang, M.; Jang, H.; Nussinov, R. PI3K inhibitors: review and new strategies. *Chem. Sci.* **2020**, *11* (23), 5855–5865.
(20) Tankova, T.; Senkus, E.; Beloyartseva, M.; Borstnar, S.; Catrinoiu, D.; Frolova, M.; Hegmane, A.; Janez, A.; Krnic, M.; Lengyel, Z.; et al. Management Strategies for Hyperglycemia Associated with the alpha-Selective PI3K Inhibitor Alpelisib for the Treatment of Breast Cancer. *Cancers (Basel)* **2022**, *14* (7).
(21) (a) Anderson, D. E.; Aronow, S. D.; Boyles, N. A.; Dahlgren, M. K; Feng,S.; Gerasyuto, A. I.; Hickey,E. R.; Irvin,C. T.;. Kesicki, E. A; Klippel-Giese, A.; Knight, J. L.; Kolakowski, G. R.; Kumar,M.; Long, K. F.; Mayne, C. G.;. Mcelligott, D. L; Mclean,A. J.; Puca, L.; Ravi, K. K.;. Severance, D. L; Welch, M. B.; Widjaja, T Allosteric Chromenone inhibitors of phosphoinositide 3-kinase (PI3K) for the treatment of diseases associated with PI3K modulation. WO2021202964, 2021. (b) Anderson, D. E.; Aronow, S. D.; Boyles, N. A. ; Chen, X.; Dawadi, S.; Hickey, E. R.; Irvin, C. T.; Kesicki, E. A.; Knight,J. L.; Kolakowski, G. R.; Kumar, M.; Long, K. F.; Mayne, C. G.; Picado, A.; Pototschnig, M. G.; Wang, H.-Y.; Welch, B. M.; Widjaja, T.; Wright, N. E. Allosteric chromenone inhibitors of phosphoinositide 3-kinase (PI3K) for the treatment of disease. WO2022235574, 2022. (c) Anderson, D. E.; Aronow, S. D.; Boyles, N. A. ; Chen, X.; Dawadi, S.; Hickey, E. R.; Irvin, C. T.; Kesicki, E. A.; Knight,J. L.; Kolakowski, G. R.; Kumar, M.; Long, K. F.; Mayne, C. G.; Picado, A.; Pototschnig, M. G.; Wang, H.-Y.; Welch, B. M.; Widjaja, T.; Wright, N. E. Allosteric chromenone inhibitors of phosphoinositide 3-kinase (PI3K) for the treatment of disease. WO2022235575, 2022. (d) Anderson, D. E.; Aronow, S. D.; Boyles, N. A.; Chen, X.; Dawadi, S.; Hickey, E. R.; Irvin, C. T.; Kesicki, E. A.; Knight, J. L.; Kolakowski, G. R.; Kumar, M.; Long, K. F.; Mayne, C. G.; Picado, A.; Pototschnig, M. G.; Wang, H.-Y.; Welch, B. M.;Widjaja, T. Allosteric chromenone inhibitors of phosphoinositide 3-kinase (PI3K) for the treatment of disease. WO2022251482, 2022. (e) Boezio, L.; Taylor, A. M.; Xhang, J.; Shortsleeves, K. C.; Pierce, L. C. T.; Mclean, T. H.; Kaplan, A.; Madec, A.; Hudson, B. M.; Ma, J.; Pan, Y.; Maertens, G.; Outin, J. PI3K-Alpha inhibitors and methods of use thereof. W02023060262, 2023. (f) Haohan, T.; Li, Z.; Liu, B.; Wang, Y.; He, C.; Liu, Q.; Xu, H.; Qi, Y.; Liu, Y.; Lin, S.; Zhao, X.; Wang, W. Compounds as protein kinase inhibitors. WO2023078401, 2023. (g) Hao, X.; Lei, Y. Fused heterocyclic compounds as PI3Kalpha inhibitors. WO2023104111, 2023. (h) Orr, S.; Tuula, M. PI3K inhibitors and methods of treating cancer. WO2023081209, 2023. (i) Cee,V. J.; Tasker, A. S.; Walton, M.; Nguyen, T.; Kubota. M. D.; Buchowiecki, P.; Toledo Warshaviak, D. Inhibitors of phosphoinositide 3-kinase (PI3K) and uses thereof. WO2023159155, 2023. (j) Chen, C.; Holmes, R.; Maity, S.; Combs, A. P.; Buesking, A. W.; Pawley, S.. Mutant PI3K-alpha inhibitors and their use as pharmaceuticals. WO2023192416, 2023. (k) Qi, C.; You, L.; Zhou, F.; Li, Y.; Zheng, H.; Bai, Y.; Pan, J.; Wu, L.; Yao, W. PI3Ka inhibitors. WO2023205680, 2023. (l) Dai, X.; Yu, Y.; Yang, H.; Yu, Y.; Huang, X.; Weng, J.; Wang, Y. Compounds, preparation methods and uses thereof. WO2023207881, 2023. (m) Zhou, F.; Qi, C.; Zheng, H.; Yang, J.; Wu, L.; Yao, W. Tricyclic compounds as PI3Kalpha inhibitors. WO2023230262, 2023. (n) Blake, J. F.; Boys, M. L.; Markeska, D. A.; Payette, J. N.; Schulte, C. A.; Yestrepsky, B.; Zhao, Q. Benzopyrimidin-4(3H)-ones as PI3K inhibitors. WO2023239710, 2023. (o) Dai, X.; Yu, Y.; Yang, H.; Yu, Y.; Huang, X.; Weng, J.; Weng, Y. Compounds, Preparation methods and uses thereof. WO2024051778, 2024. (p) Blake, J. F.; Boys, M. L.; Mareska, D. A.; Payette, J. N.; Schulte, C. A.; Yestrepsky, B.; Zhang, Q. Isoquinolones as PI3K inhibitors. WO2024054469, 2024. (q) Blake,J. F.; Boys,M. L.; Mareska, D. A.; Payette, J. N.; Schulte, C. A.; Yestrepsky, B.; Zhang, Q. ((4-oxo-3,4-dihydroquinazolin-8-yl)methyl)amine derivatives as PI3K inhibitors for the treatment of cancer. WO2024064024, 2024.(22) (a) Wailes, P. C.; Weigold, H. Hydrido complexes of zirconium I. Preparation. *J. Organomet. Chem.* **1970**, *24* (2), 405–411. (b) Wailes, P. C.; Weigold, H.; Bell, A. P. Hydrido complexes of zirconium. *J. Organomet. Chem.* **1971**, *27* (3), 373–378.

(23) (a) Schwartz, J.; Labinger, J. A. Hydrozirconation: A New Transition Metal Reagent for Organic Synthesis. *Angew. Chem. Int. Ed. Eng.* **1976**, *15* (6), 333–340. (b) Hart, D. W.; Schwartz, J. Hydrozirconation. Organic synthesis via organozirconium intermediates. Synthesis and rearrangement of alkylzirconium(IV) complexes and their reaction with electrophiles. *J. Am. Chem. Soc.* **2002**, *96* (26), 8115–8116.
(24) Aloiau, A. N.; Bobek, B. M.; Caddell Haatveit, K.; Pearson, K. E.; Watkins, A. H.; Jones, B.; Smith, C. R.; Ketcham, J. M.; Marx, M. A.; Harwood, S. J. Stereoselective Amine Synthesis Mediated by a Zirconocene Hydride to Accelerate a Drug Discovery Program. *J. Org. Chem.* **2024**, *89* (6), 3875–3882.
(25) (a) Liu, G.; Cogan, D. A.; Ellman, J. A. Catalytic Asymmetric Synthesis of tert-Butanesulfinamide. Application to the Asymmetric Synthesis of Amines. *J. Am. Chem. Soc.* **1997**, *119* (41), 9913–9914. (b) Liu, G.; Cogan, D. A.; Owens, T. D.; Tang, T. P.; Ellman, J. A. Synthesis of Enantiomerically Pure N-tert-Butanesulfinyl Imines (tert-Butanesulfinimines) by the Direct Condensation of tert-Butanesulfinamide with Aldehydes and Ketones. *J. Org. Chem.* **1999**, *64* (4), 1278–1284. (c) Ellman, J. A.; Owens, T. D.; Tang, T. P. N-tert-butanesulfinyl imines: versatile intermediates for the asymmetric synthesis of amines. *Acc. Chem. Res.* **2002**, *35* (11), 984–995. (d) Robak, M. T.; Herbage, M. A.; Ellman, J. A. Synthesis and applications of tert-butanesulfinamide. *Chem. Rev.* **2010**, *110* (6), 3600–3740.
(26) For a definition of chemoselectivity see: Shenvi, R. A.; O'Malley, D. P.; Baran, P. S. Chemoselectivity: the mother of invention in total synthesis. *Acc. Chem. Res.* **2009**, *42* (4), 530–541.
(27) For a definition of divergent synthesis see: (a) Boger, D. L.; Brotherton, C. E. Total synthesis of azafluoranthene alkaloids: rufescine and imeluteine. *J. Org. Chem.* **1984**, *49* (21), 4050–4055. (b) Li, L.; Chen, Z.; Zhang, X.; Jia, Y. Divergent Strategy in Natural Product Total Synthesis. *Chem. Rev.* **2018**, *118* (7), 3752–3832.
(28) For a definition of synthetic strategy and synthetic tactic see: Smith, J. M.; Harwood, S. J.; Baran, P. S. Radical Retrosynthesis. *Acc. Chem. Res.* **2018**, *51* (8), 1807–1817.
(29) Anastas, P. T.; Bartlett, L. B.; Kirchhoff, M. M.; Williamson, T. C. The role of catalysis in the design, development, and implementation of green chemistry. *Catalysis Today* **2000**, *55* (1–2), 11–22.
(30) Peng, L.; Zhao, Y.; Yang, T.; Tong, Z.; Tang, Z.; Orita, A.; Qiu, R. Zirconium-Based Catalysts in Organic Synthesis. *Top. Curr. Chem. (Cham)* **2022**, *380* (5), 41.
(31) Anselm, M. B., L.; Brintzinger, H. H.; Cui, L.; Fischer, D.; Hakala, K.; Halbach, T.; Kaminsky, W.; Kukko, E.; Kurek, A.; Lehmus, P.; Lipponen, S.; Lofgren, B.; Luinstra, G. A.; Meyer, R. S. A.; Mike Chung, T. C.; Mulhaupt, R.; Pakkanen nee Malmberg, A; Razavi, A.; Seppala, J.; Hiono,T.; Sinn, H.; Sun W.-H.; Sturzel, M.; Tarte, N.H.; Tritto, I.; Woo, S. . *Polyolefins: 50 years after Ziegler and Natta II*; 2013.

(32) Xu, S.; Negishi, E. I. Zirconium-Catalyzed Asymmetric Carboalumination of Unactivated Terminal Alkenes. *Acc. Chem. Res.* **2016**, *49* (10), 2158–2168.
(33) (a) Negishi, E.-i.; Yoshida, T. A novel zirconium-catalyzed hydroalumination of olefins. *Tetrahedron Lett.* **1980**, *21* (16), 1501-1504. (b) Makabe, H.; Negishi, E.-i. Hydrogen Transfer Hydrozirconation of Alkenes with iBuZrCp2Cl Catalyzed by Lewis-Acidic Metal Compounds Containing Al, Zn, Si, Ag, and Pd. *Euro. J. Org. Chem.* **1999**, *1999* (5), 969–971. (c) Parfenova, L. V.; Pechatkina, S. V.; Khalilov, L. M.; Dzhemilev, U. M. Mechanism of Cp2ZrCl2-catalyzed olefin hydroalumination by alkylalanes. *Russ. Chem. Bull.* **2005**, *54* (2), 316–327. (d) Andrews, P.; Latham, C. M.; Magre, M.; Willcox, D.; Woodward, S. ZrCl2(eta-C5Me5)2-AlHCl2.(THF)2: efficient hydroalumination of terminal alkynes and cross-coupling of the derived alanes. *Chem. Commun. (Camb)* **2013**, *49* (15), 1488–1490.
(34) Takahashi, T.; Suzuki, N.; Kageyama, M.; Nitto, Y.; Sabur, M.; Negishi, E.-i. Catalytic Hydrogenation of Alkenes Using Zirconocene–Alkene Complexes. *Chem. Lett.* **1991**, *20* (9), 1579–1582.
(35) (a) Willoughby, C. A.; Buchwald, S. L. Synthesis of highly enantiomerically enriched cyclic amines by the catalytic asymmetric hydrogenation of cyclic imines. *J. Org. Chem.* **1993**, *58* (27), 7627–7629. (b) Carter, M. B.; Schiott, B.; Gutierrez, A.; Buchwald, S. L. Enantioselective Hydrosilylation of Ketones with a Chiral Titanocene Catalyst. *J. Am. Chem. Soc.* **1994**, *116* (26), 11667–11670. (c) Willoughby, C. A.; Buchwald, S. L. Catalytic Asymmetric Hydrogenation of Imines with a Chiral Titanocene Catalyst: Kinetic and Mechanistic Investigations. *J. Am. Chem. Soc.* **1994**, *116* (26), 11703–11714. (d) Verdaguer, X.; Lange, U. E. W.; Reding, M. T.; Buchwald, S. L. Highly Enantioselective Imine Hydrosilylation Using (S,S)-Ethylenebis(η5-tetrahydroindenyl)titanium Difluoride. *J. Am. Chem. Soc.* **1996**, *118* (28), 6784–6785. (e) Verdaguer, X.; Hansen, M. C.; Berk, S. C.; Buchwald, S. L. Titanocene-Catalyzed Reduction of Lactones to Lactols. *J. Org. Chem.* **1997**, *62* (24), 8522-8528. (f) Verdaguer, X.; Lange, U. E. W.; Buchwald, S. L. Amine Additives Greatly Expand the Scope of Asymmetric Hydrosilylation of Imines. *Angew. Chem. Int. Ed.* **1998**, *37* (8), 1103–1107. (g) Yun, J.; Buchwald, S. L. Titanocene-Catalyzed Asymmetric Ketone Hydrosilylation: The Effect of Catalyst Activation Protocol and Additives on the Reaction Rate and Enantioselectivity. *J. Am. Chem. Soc.* **1999**, *121* (24), 5640–5644. (h) Takahashi, K.; Ogiwara, Y.; Sakai, N. Palladium-Catalyzed Reductive Coupling Reaction of Terminal Alkynes with Aryl Iodides Utilizing Hafnocene Difluoride as a Hafnium Hydride Precursor Leading to trans-Alkenes. *Chem. Asian. J.* **2018**, *13* (7), 809–814.
(36) Takahashi, K.; Morishita, H.; Ogiwara, Y.; Sakai, N. Group 4 Metallocene Difluoride/Palladium Bimetallic Catalysts for the Reductive Cross-Coupling of Alkynes with Aryl Iodides and Bromides. *J. Org. Chem.* **2018**, *83* (22), 13734–13742.
(37) (a) Kehner, R. A.; Hewitt, M. C.; Bayeh-Romero, L. Expanding Zirconocene Hydride Catalysis: In Situ Generation and Turnover of ZrH Catalysts Enabling Catalytic Carbonyl Reductions. *ACS Catal.* **2022**, *12* (3), 1758–1763. (b) Kobylarski, M.; Donnelly, L. J.; Berthet, J.-C.; Cantat, T. Zirconium-catalysed hydrosilylation of esters and depolymerisation of polyester plastic waste. *Green Chemistry* **2022**, *24* (18), 6810–6815. (c) Kehner, R. A.; Lubaev, A. E.; Rathnayake, M. D.; Loden, R.; Zhang, G.; Bayeh-Romero, L. Selective zirconocene hydride-catalyzed semi-hydrogenation of terminal alkynes. *Tetrahedron* **2023**, *133*. (d) Kehner, R. A.; Zhang, G.; Bayeh-Romero, L. Mild Divergent Semireductive Transformations of Secondary and Tertiary Amides via Zirconocene Hydride Catalysis. *J. Am. Chem. Soc.* **2023**, *145* (9), 4921–4927.
(38) (a) Magnus, P.; Fielding, M. R. Acceleration of the reduction of aldehydes and ketones using Mn(dpm)3 catalyst and phenylsilane in the presence of dioxygen. *Tetrahedron Lett.* **2001**, *42* (38), 6633–6636. (b) Obradors, C.; Martinez, R. M.; Shenvi, R. A. Ph(i-PrO)SiH2: An Exceptional Reductant for Metal-Catalyzed Hydrogen Atom Transfers. *J. Am. Chem. Soc.* **2016**, *138* (14), 4962–4971.
(39) (a) Furin, G. G.; Vyazankina, O. A.; Gostevsky, B. A.; Vyazankin, N. S. Tetrahedron report number 234 Synthetic aspects of the use of organosilicon compounds under nucleophilic catalysis conditions. *Tetrahedron* **1988**, *44* (10), 2675-2749. (b) Chuit, C.; Corriu, R. J. P.; Reye, C.; Young, J. C. Reactivity of penta- and hexacoordinate silicon compounds and their role as reaction intermediates. *Chem. Rev.* **2002**, *93* (4), 1371–1448.
(40) (a) Kelly, R. W.; McClenaghan, I.; Sykes, P. J. Synthetic steroids. II. The deconjugation of delta-4-3-oxo-steroids. An improved method for the preparation of 3-beta-hydroxyandrost-5-ene-11,17-dione. *J. Chem. Soc. Perkin 1* **1967**, *22*, 2375–2381. (b) Morreal, C. E.; Synthesis of androst-4-en-3β-Ol-11,17-dione. *Steroids*. **1966**, *8* (5), 671-677.
(41) Dauben, W. G.; Fonken, G. J.; Noyce, D. S. The Stereochemistry of Hydride Reductions. *J. Am. Chem. Soc.* **1956**, *78* (11), 2579–2582.
(42) Colyer, J. T.; Andersen, N. G.; Tedrow, J. S.; Soukup, T. S.; Faul, M. M. Reversal of diastereofacial selectivity in hydride reductions of N-tert-butanesulfinyl imines. *J. Org. Chem.* **2006**, *71* (18), 6859–6862.
(43) MacNevin, C. J.; Atif, F.; Sayeed, I.; Stein, D. G.; Liotta, D. C. Development and screening of water-soluble analogues of progesterone and allopregnanolone in models of brain injury. *J. Med. Chem.* **2009**, *52* (19), 6012–6023.
(44) Li, H.-Y. S., Haoran; DiMagno, Stephen G. Tetrabutylammonium Fluoride. *Encyclopedia of reagents for Organic Synthesis* **2007**.
(45) Corriu, R. J. P.; Perz, R.; Reye, C. Activation of silicon-hydrogen, silicon-oxygen, silicon-nitrogen bonds in heterogeneous phase. *Tetrahedron*. **1983**, *39* (6), 999-1009.
(46) Watson, L. A.; Yandulov, D. V.; Caulton, K. G. C-D(0) (D(0) = pi-donor, F) Cleavage in H(2)C=CH(D(0)) by (Cp(2)ZrHCl)(n): mechanism, agostic fluorines, and a carbene of Zr(IV). *J. Am. Chem. Soc.* **2001**, *123* (4), 603–611.
(47) Reid, A. F.; Shannon, J. S.; Swan, J. M.; Wailes, P. C. Characterization of Bis[chloridodi(cyclopentadienyl)zirconium] oxide, a compound containing the Zr-O-Zr linkage. *Aus. J. Chem.* **1965**, *18* (2).
(48) Marek, I. *Titanium and Zirconium in Organic Synthesis*; 2002.
(49) Majoral, J.-P.; Zablocka, M. Zirconate complexes: multifaceted reagents. *New J. Chem.* **2005**, *29* (1).